ICMIEE-PI-140333

Laminar Boundary Layer Flow Separation Control at the Leading Edge of an Airfoil

G.M Hasan Shahariar[1], Mohammad Rashedul Hasan[2], Dr. Mohammad Mashud[3]

[1,2,3] Department of Mechanical Engineering,
Khulna University of Engineering & Technology, Khulna-9203, BANGLADESH

ABSTRACT
In this paper, laminar boundary layer flow separation control at the leading edge of two dimensional NACA 2412 airfoil is investigated numerically through a commercial fluid dynamic code ANSYS FLUENT and to study the effects of laminar separation bubble on airfoil aerodynamic characteristics. Flow was fully turbulent with the Reynolds number of 6.85×10^5 and For these flows, the Reynolds Average Navier-Stokes equation with k-ω SST transition model are shown to accurately predict the characteristics of laminar separation bubble. In the present case, a flap with a length of 4% the camber at a distance of 12% the chord length from the leading edge is placed on the airfoil's upper surface at an angle of 5, 10, 15 degree. The numerical simulation reveals details of the actuation in modifying the leading edge flow giving insight in the induced effect by using flap. The effectiveness of the flap is observed in a wide range of angles of attack with lift co-efficient, drag co-efficient and surface pressure distribution of the airfoil.

Key Words
Laminar separation bubble, Flow separation control, CFD, Airfoil, Flap, RANS;

1. Introduction

The performance of almost all model aircraft is strongly influenced by laminar separation bubbles, which may occur at low Reynolds numbers. Such a separation bubble is caused by a strong adverse pressure gradient, which makes the laminar boundary layer to separate from the curved airfoil surface. The pressure rise is related to the velocity drop towards the trailing edge of the airfoil, which can be seen in the velocity distribution of the airfoil through Bernoulli's equation.

The boundary layer leaves the surface approximately in tangential direction, resulting in a wedge shaped separation area. The separated, but still laminar flow is highly sensitive to disturbances, which finally cause it to transition to the turbulent state. The transition region is located away from the airfoil at the outer boundary of the separated flow area. The thickness of the now turbulent boundary layer grows rapidly, forming a turbulent wedge, which may reach the airfoil surface again. The region where the turbulent flow touches the surface again is called reattachment point. The volume enclosed by the regions of separated laminar flow and turbulent flow is called a laminar separation bubble. Inside the bubble the flow may be circulating, the direction near the airfoil surface may even be the opposite of the direction of the outer flow. There is almost no energy exchange with the outer flow, which makes the laminar separation bubble quite stable.

The laminar separation bubble on the airfoil is classified into a short bubble and a long bubble. With increasing angle of attack, the chordwise length of the short bubble shortens and its position moves toward the leading edge. With further increase in the angle of attack, the short bubble fails to reattach on the airfoil surface, which is known as a short bubble burst and this bubble burst causes the airfoil stall. The long bubble, which is formed after the burst, increases its chord wise length as the angle of attack is increased beyond the stall angle. The stall characteristics of the airfoil are strongly dependent upon these two types of bubbles. The negative pressure peak near the leading edge is observed when the short bubble is formed. When the long bubble is formed after the bubble burst, this negative pressure peak is destroyed and a relatively flattened pressure distribution is formed. [1]

Recent improvements on airfoil performance were achieved by increasing the maximum lift and suppressing the stall. Many investigations on the airfoil flow control have been conducted. Some classical devices such as a leading-edge slat and a vortex generator [2] have been developed as passive control devices to control the airfoil lift. Recently, active control devices such as a jet blowing into the boundary layer [3] and oscillatory actuators and synthetic jet actuators [4] have been investigated. And many other investigations have been conducted. Another way to control the flow separation near the trailing edge is by the use of trailing-edge flap actuation [5].

However, both passive and active lift control devices were designed for the suppression of boundary-layer separation and they were not aimed for the control of the behavior of the bubble formed near the leading edge. In this paper, the control of the bubble formed on the NACA 2412 airfoil with the application of flap is pursued.

2. Numerical Method

In this study, laminar flow separation control at the leading edge over NACA 2412 airfoil is computationally investigated using computational fluid dynamics (CFD) code with commercial ANSYS Fluent 14.5 software based on finite volume technique. Here, the chord length

E-mail addresses: hasanshahariar.kuet@gmail.com, rashedulhasan.047@gmail.com , mdmashud@yahoo.com

of the airfoil is 1m. NACA 2412 airfoil has a maximum camber of 2% located 40% (0.4 chords) from the leading edge with a maximum thickness of 12% of the chord. Reynolds number for the simulations was $Re=6.85\times10^6$. The density of the air at the given temperature is $\rho=1.225kg/m^3$ and the viscosity is $\mu=1.7894\times10^{-5}kg/ms$. A flap with a length of 4% the camber at a distance of 12% the chord length from the leading edge is placed on the airfoil's upper surface at an angle of 5, 10, 15 degree respectively. The numerical simulation was done for NACA 2412 airfoil with and without flap at an angle of attack from 0 degree to 16 degree at a wind velocity of 10 m/s. The Reynolds average Navier-Stokes equations ware solved using the green gauss cell based gradient option and the IMPLICIT density based solver was selected with a second order implicit transient formulation for improved accuracy. The turbulent viscosity was computed through k-ω SST transition model. All solution variables were solved via second order upwind discretization scheme.

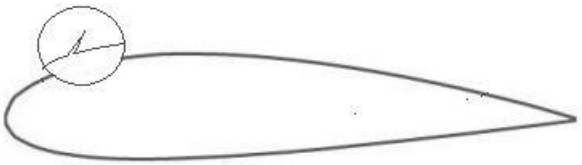

Fig.1 NACA 2412 airfoil with flap at the leading edge

2.1 Boundary Condition:
The computational domain extended 15C upstream of the leading edge of the airfoil, 15C downstream of the trailing edge, and 20C above the pressure surface. Velocity inlet boundary condition was applied upstream (Inflow) with speed of (U=10 m/sec) and outflow boundary condition was applied downstream. Free stream boundary conditions are used in the upstream, downstream and outer boundaries. No-slip boundary conditions are used at solid surfaces.

It involves inlet, outlet & wall boundary, the velocity components are calculated for each angle attack case as follows. The x component of velocity is calculated by $x=u\cos\alpha$ and the y component of velocity is calculated by $y=y\sin\alpha$, where α is the angle of attack in degrees. Ansys recommends turbulence intensities ranging from 1% to 5% as inlet boundary conditions. In this study it is assumed that inlet velocity is less turbulent that pressure outlet. Hence, for velocity inlet boundary condition turbulence intensity is considered 1% and for pressure outlet boundary 5%. In addition, Ansys also recommends turbulent viscosity ratio of 10 for better approximation of the problem [6].

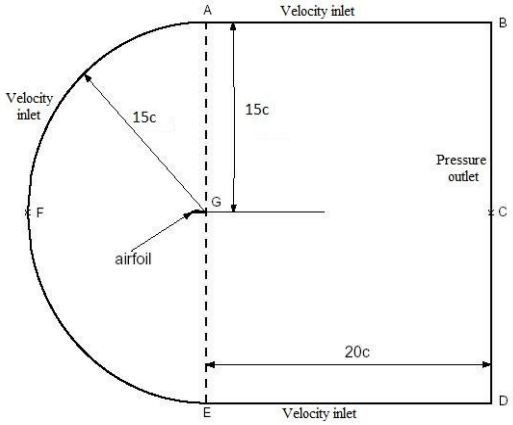

Fig.1 The dimensions and boundary conditions of the computational domain

2.2 Mesh Topology:
The grid used for the single airfoil is generated by the GAMBIT program, and is shown in Figure 2. The application of wall functions to modeling the near-wall region may significantly reduce both the processing and storage requirements of a numerical model, while producing an acceptable degree of accuracy. The non-dimensional wall parameter is defined as:

$$y^+ = \frac{\rho y_p}{\mu}\sqrt{\frac{\tau_\omega}{\rho_\omega}} \qquad (1)$$

Here, y_p is the distance from the first computational node to the wall and the subscript ω denotes wall properties [4]. Consequently, the grid size giving the grid independent results are selected and the total number of cells is adopted as 45,297 nodes. For solution convergence criteria was selected as 1^{0-5}.This indicates the value taken as the result were constant for consecutive 2000 iterations. Other criterions like continuity residuals were also monitored.

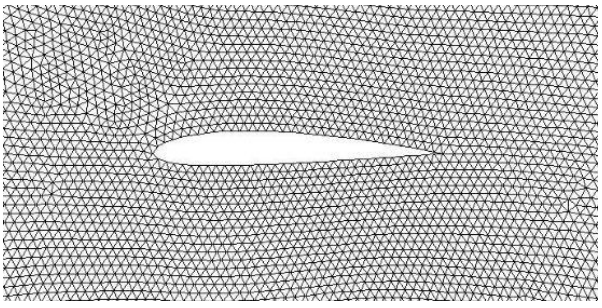

Fig.3 Mesh around NACA 2412

E-mail addresses: hasanshahariar.kuet@gmail.com, rashedulhasan.047@gmail.com , mdmashud@yahoo.com

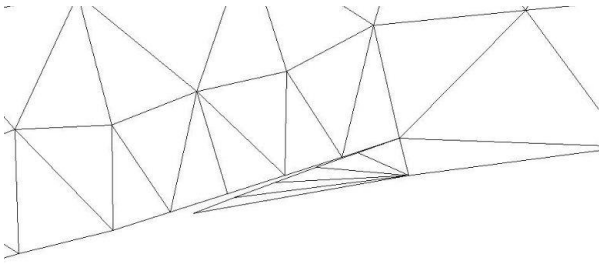

Fig.4 Mesh near the flap at 10 degree flap angle

2.3 Grid independence study:

The first step in performing a CFD simulation should be to investigate the effect of the mesh size on the solution results. Generally, a numerical solution becomes more accurate as more nodes are used, but using additional nodes also increases the required computer memory and computational time. The appropriate number of nodes can be determined by increasing the number of nodes until the mesh is sufficiently fine so that further refinement does not change the results. Figure 5 shows the effect of number of grid cells in coefficient of lift at stall angle of attack (16°). This computational model is very small compared to that of NASA's validation cases.

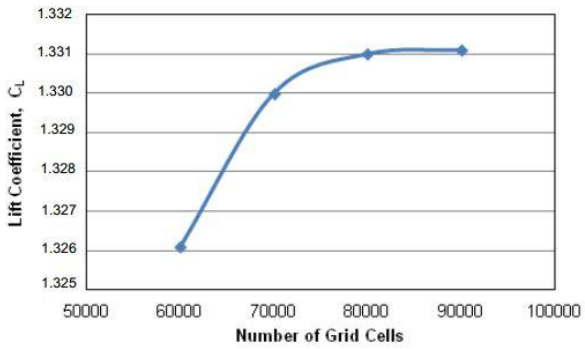

Fig.5 Variation of lift coefficient with number of grid cells [7]

3. Results & Discussions:

Figure 6 shows the lift coefficient (C_l) versus angle of attack (α) curve of NACA 2412 airfoil with a flap angle of 5, 10, 15 degree and compares them with the NACA 2412 airfoil without flap at a wind velocity of 10 m/s. The maximum lift coefficient defines the angle at which the airfoil will stall and the stall occurred at the angle of attack of 11° where $C_{l,max}$= 0.841. The graph depicted in figure 3 also shows the drag coefficient variations with the angle of attack. Here, the drag co-efficient increases as the increase of angle of attack of wind velocity.

From the both curve it is found that the airfoil performance is significantly improved due to the control of flow separation by using flap at the leading edge. It has also been found that the lift increases about 20.6% & 13.27% and drag reduces about 26.12% & 19.55% at the flap angle 5 & 10 degree respectively for 10 degree

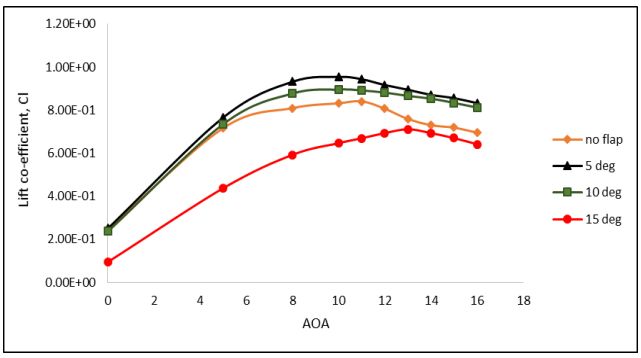

Fig.6 Lift co-efficient vs angle of attack at 10 m/s

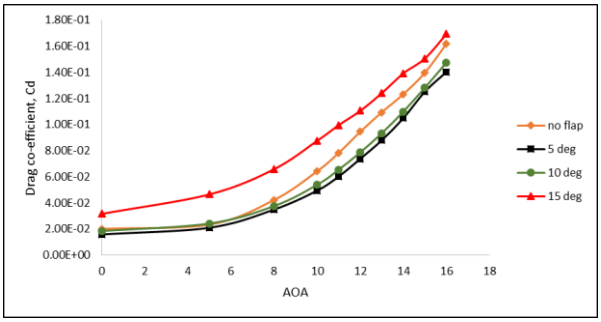

Fig.7 Drag co-efficient vs angle of attack at 10 m/s

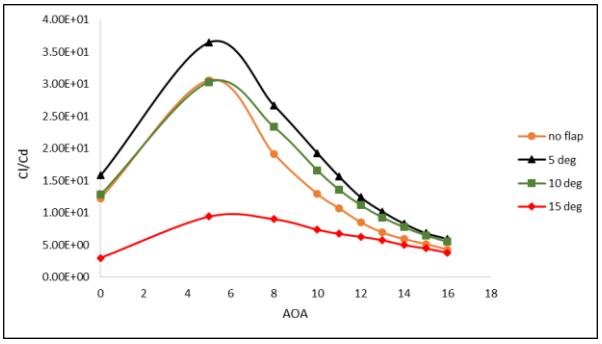

Fig.8 Lift-Drag ratio vs angle of attack at 10 m/s

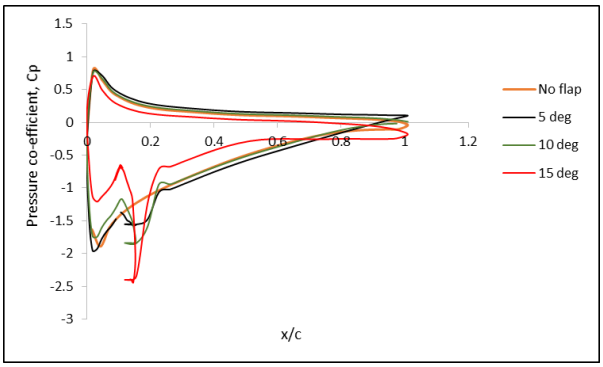

Fig.9 Surface pressure distribution over the airfoil at 8 degree angle of attack

angle of attack. Because of attaching flap at the leading edge, there formed bubbles which create so much negative pressure on the upper surface of the airfoil. Thus the reattachment of flow happened rapidly which

E-mail addresses: hasanshahariar.kuet@gmail.com, rashedulhasan.047@gmail.com , mdmashud@yahoo.com

reduces the flow separation region. As a result lift co-efficient increases and drag co-efficient decreases. But at 15 degree flap angle, lift reduces about 18.2% and drag increases about 30.75% at 10 degree angle of attack. From figure 8 it also seen that the lift to drag ratio is increases about 49.61% & 28.68% at flap angle of 5 & 10 degree respectively for 10 degree angle of attack but it decreases about 42.8% at 15 degree flap angle for the same angle of attack than the clean airfoil. Figure 9 shows the surface pressure distribution along the chord wise position of the airfoil with and without flap at 8 degree angle of attack.

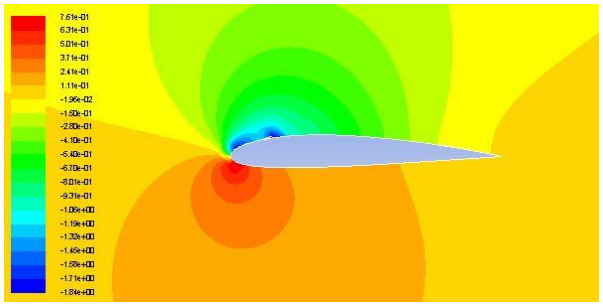

Fig.10 Pressure contours of NACA 2412 with 10 degree flap angle at 8 degree angle of attack

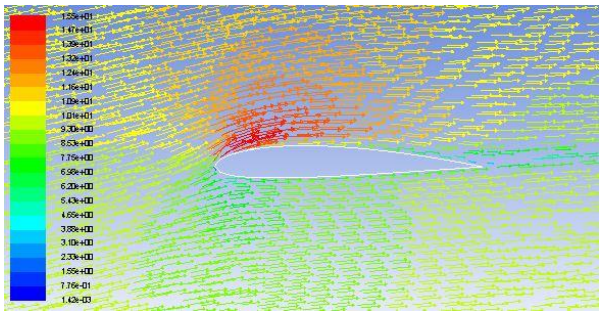

Fig.11 Velocity vector around NACA 2412 with 5 degree flap angle at 8 degree angle of attack

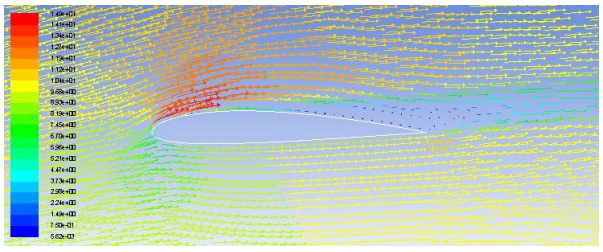

Fig.12 Velocity vector around NACA 2412 with 15 degree flap angle at 8 degree angle of attack

Figure 10 shows the contours of pressure at a flap angle of 10 degree for 8 degree angle of attack. It also seen from the figure 11 & 12 that, at 5 degree flap angle the flow separation region is quite smooth and short than 15 degree for 8 degree angle of attack. So, there have been found a better aerodynamics characteristics for NACA 2412 airfoil with 5 degree flap angle.

4. Conclusion:

For the purpose of burst suppression of the laminar separation bubble, flaps are tested on the NACA 2412 airfoil for different flap angles at a Reynolds number of 6.85×10^5.

- The results indicates that the burst of the bubble is suppressed and both the maximum lift coefficient and the stall angle are improved when the burst control plate (flap) is at an appropriate position (flap angle 5 degree).
- It has also been found that the lift increases about 20.6% & 13.27% and drag reduces about 26.12% & 19.55% at the flap angle 5 & 10 degree respectively for 10 degree angle of attack. Thus it can be strongly recommended to use bubble burst control mechanism to increase the aerodynamics performance of airfoil.

NOMENCLATURE

C_p : Pressure co-efficient over the airfoil surface
C_l : Lift co-efficient
C_d : Drag co-efficient
α : Angle of attack
μ : Dynamic viscosity
ρ : Air density
RANS: Reynolds Average Navier Stokes equation
C_l/C_d: Lift to Drag ratio
NACA: National Advisory Committee for Aeronautics

REFERENCES

[1] Kenichi Rinoie, Masafumi Okuno, and Yasuto Sunada, “Airfoil Stall Suppression by Use of a Bubble Burst Control Plate”, AIAA JOURNAL, Vol. 47, No. 2, February 2009

[2] Bragg, M. B., Gregorek, G. M., “Experimental Study of Airfoil Performance with Vortex Generators,” Journal of Aircraft, Vol. 24, No. 5, 1987

[3] Huang, L., Huang, P. G., LeBeau, R. P., and Hauser, T., “Numerical Study of Blowing and Suction Control Mechanism on NACA0012 Airfoil,” Journal of Aircraft, Vol. 41, No. 5, 2004

[4] Munday, D., Jacob, J. D., and Huang, G., “Active Flow Control of Separation on a Wing with Oscillatory Camber,” AIAA Paper 2002- 0413, 2002

[5] Melton, L. P., Yao, C. S., and Seifert, A., “Active Control of Separation from the Flap of a Supercritical Airfoil,” AIAA Journal, Vol. 44, No. 1, 2006

[6] Wilcox, David C, "Turbulence Modeling for CFD", Second edition, Anaheim, DCW Industries, 1998.

[7] Eleni, Douvi C., Tsavalos I. Athanasios, and Margaris P. Dionissios. "Evaluation of the turbulence models for the simulation of the flow over a National Advisory Committee for Aeronautics (NACA) 0012 airfoil." Journal of Mechanical Engineering Research 4.3 (2012): 100-111

E-mail addresses: hasanshahariar.kuet@gmail.com, rashedulhasan.047@gmail.com , mdmashud@yahoo.com